nature nanotechnology

REVIEW ARTICLE

PUBLISHED ONLINE: 6 JANUARY 2014 | DOI: 10.1038/NNANO.2014.271

Silicon nanostructures for photonics and photovoltaics

Francesco Priolo[1,2,3]*, Tom Gregorkiewicz[4], Matteo Galli[5] and Thomas F. Krauss[6]

Silicon has long been established as the material of choice for the microelectronics industry. This is not yet true in photonics, where the limited degrees of freedom in material design combined with the indirect bandgap are a major constraint. Recent developments, especially those enabled by nanoscale engineering of the electronic and photonic properties, are starting to change the picture, and some silicon nanostructures now approach or even exceed the performance of equivalent direct-bandgap materials. Focusing on two application areas, namely communications and photovoltaics, we review recent progress in silicon nanocrystals, nanowires and photonic crystals as key examples of functional nanostructures. We assess the state of the art in each field and highlight the challenges that need to be overcome to make silicon a truly high-performing photonic material.

Crystalline silicon (c-Si) is the most important semiconductor material for the electronics and photovoltaics industries today, and it has become the cornerstone of our knowledge-based society. This prominent position follows from a unique combination of advantageous properties: the availability of large single crystals, high purity, effective conductivity engineering, a matching insulator and, very importantly, natural abundance. These properties have enabled the electronics industry to follow Moore's law for over four decades, which is truly remarkable and which has driven the development of silicon technology to its present maturity. Together with its 1.1-eV bandgap — optimal for capturing the solar spectrum using a single-junction device — this maturity makes silicon almost ideally suited for photovoltaics applications. As a result, around 90% of solar panels in use today are based on silicon.

The optical properties of c-Si are relatively poor, owing to its indirect bandgap which precludes the efficient emission and absorption of light. This is a considerable weakness, especially given that some properties of c-Si are already very good, as illustrated, for example, by the successful realization of Raman lasing[1–4] and the demonstration of ultrafast electro-optic modulation[5,6]. High performance in all aspects of optical functionality is highly desired, as it would enable true optoelectronic integration and pave the way to faster, highly integrated and low-cost devices. For photovoltaics applications, higher optoelectronic performance would be the much-desired enabler of a new generation of high-efficiency thin-film Si solar cells. We believe that nanostructures offer a range of opportunities for all of these application areas and that nanostructures herald a new era of silicon photonics and photovoltaics.

Silicon nanostructures for communications

Optical signals are now well established as a means for efficient data transfer from very long (Internet) to very short (rack-to-rack) distances. On-chip data processing is still being performed electronically, however, even though processor clock speeds have been limited by the interconnect problem for a number of years[7]. The next step-change is to introduce photonics into on-chip communications, which requires nanoscale optical sources, circuits and detectors to encode and transmit data around the chip. Silicon is poised to deliver this functionality, as silicon photonic devices are CMOS-compatible, and many highly performing devices have already been demonstrated[1–12]. Photonic crystal nanostructures add unique capabilities to this toolkit, as they offer extremely tight light confinement, thus providing strongly enhanced nonlinear effects already for microwatt pump power levels[8,9], modulators with very low (femtojoule per bit level) switching energy[10,11] and the opportunity for enhancing and suppressing spontaneous emission[12].

In addition to nanostructuring, many material engineering options have been explored, such as the alloying of silicon and germanium[13], doping[14,15], strain and defect engineering[16,17]. Arguably the most successful way to manipulate the energy structure of Si, however, is to use quantum confinement in nanostructures[18]. Semiconductor nanostructures — nanocrystals and nanowires — are widely investigated in view of their exciting physical properties and with an eye to possible optoelectronic, photonic and photovoltaic applications. In particular, owing to the modification of the energy structure afforded by quantization, semiconductor nanocrystals emerge as ideal candidates for photonic applications involving efficient radiative recombination. The best examples highlighting the advantages of quantization of direct-bandgap semiconductors are quantum dots[19,20], with quantization in silicon offering similar benefits, as we will explore next.

Nanocrystals and nanowires. Silicon nanocrystals have been studied intensively over the past decade[21,22]. Most notably, it has been established that the excitonic emission from Si nanocrystals has two characteristic features: with decreasing crystal size, the spectrum shifts to the blue and its intensity increases. This observation indicates the quantization-related increase of the bandgap and the enhancement of the radiative recombination rate, as momentum conservation is gradually relaxed with reducing grain size owing to the Heisenberg principle[23], while the transition itself remains indirect. Further, a possible participation of oxygen and/or interface-related states has been suggested that leads to a stabilization of the photoluminescence wavelength for Si nanocrystals smaller than 3 nm in diameter[24–26]. See Box 1 for a review of the fabrication methods and Box 2 for a summary of the properties of Si nanocrystals.

[1]Scuola Superiore di Catania, Università di Catania, via Valdisavoia 9, 95123 Catania, Italy, [2]Dipartimento di Fisica e Astronomia, Università di Catania, via S. Sofia 64, 95123 Catania, Italy, [3]MATIS IMM-CNR, via S. Sofia 64, 95123 Catania, Italy, [4]Van der Waals-Zeeman Institute, University of Amsterdam, Science Park 904, 1098 XH Amsterdam, The Netherlands, [5]Dipartimento di Fisica, Università di Pavia, via Bassi 6, 27100 Pavia, Italy, [6]Department of Physics, University of York, York YO10 5DD, UK. *e-mail: francesco.priolo@ct.infn.it

Box 1 | Fabrication of Si nanostructures.

The most successful methods for fabricating silicon nanocrystals are self-assembly from silicon-rich silicon oxide matrices[150–152], plasma synthesis[101–105], and colloidal chemistry[153–156]. In the first case, SiO_x (with $x < 2$) is formed by a thin-film deposition technique such as magnetron sputtering or chemical vapour deposition, or by implantation of an SiO_2 layer with a high dose of silicon ions. Subsequent high-temperature annealing of the substoichiometric film (typically above 800 °C) produces a phase separation between Si and SiO_2 with the formation of Si nanoclusters that grow by Ostwald ripening (panel **a**). The dimensions, crystallinity and size distribution of the nanoclusters depend on the Si excess, the temperature and the annealing time[150,151].

A variation of this method is to form a superlattice of alternating SiO_x and SiO_2 layers. In this case, the precipitation of Si nanoclusters in the SiO_x layers can be controlled to a much narrower size distribution through the thickness of the SiO_x film[152]. Plasma processing is of special interest here, as it offers the prospect of scaling up, which makes the approach particularly suitable for photovoltaic applications[101,105]. Colloidal solutions of Si nanocrystals can be made from freestanding porous Si (refs 153,154) or plasma-synthesized powders[155], or synthesized directly using the sol–gel method or a variety of wet-chemical processes[156]. Especially interesting properties have recently been reported[48,49] for colloidal Si nanocrystal prepared by a wet-chemical oxidation–reduction method adapted from ref. 157 (panel **b**). This type of synthesis yields photostable and freestanding *n*-butyl-terminated Si nanocrystals of typically 2–3 nm in diameter. In general, one can conclude that Si nanocrystals prepared by precipitation in SiO_x layers are characterized by the largest tunability range and the best stability and quantum yield of emission, whereas the colloids offer the potential up-scaling for large volumes and the advantage of low-temperature processing.

Silicon nanowires can also be made by several preparation methods, most notably (i) nanolithography, (ii) the vapour–liquid–solid (VLS) method and (iii) metal-assisted chemical etching (MACE). Nanolithographic pillars are formed with a mask and a highly anisotropic reactive ion etching process. These pillars are typically too big to show quantum confinement effects, so they are usually thinned by oxidation followed by an etching process[55,56]. In the VLS method[50], metal droplets (typically gold) are formed on a silicon surface by lithography or self-assembly. These droplets are heated to temperatures above the Au–Si eutectic point (T_E) while a background flux of Si is provided by methods such as chemical vapour deposition, electron-beam evaporation or molecular beam epitaxy. The Au droplets become saturated with Si atoms, and nanowires then grow below the droplet with the droplet being pushed up (panel **c**)[158]. In the third method (MACE), the entire process occurs at room temperature, which avoids any metal diffusion. A metal salt is usually used to catalyse silicon etching within an aqueous H_2O_2/HF solution[57,58,159]. This typically forms metallic dendrite structures on top of the nanowires, which can be removed but result in damage to the nanowires. A better method is to etch using an ultrathin metallic film in place of the metal salts[59–61]. Silicon is oxidized and etched below the metal, and the small regions uncovered by the metal represent the precursors for nanowire formation. These regions (and in turn the nanowire size) can be modified by changing the thin-film thickness and taking advantage of the film roughness. This provides a powerful maskless method for nanowire formation[60] (panel **d**).

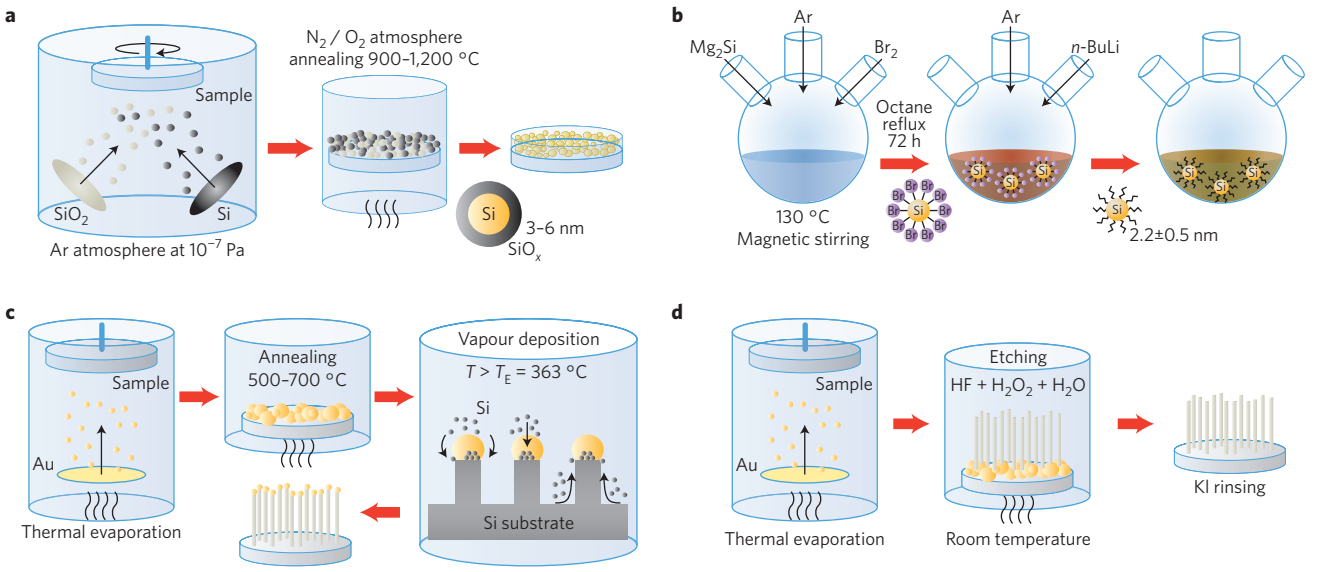

For light emission applications, Si nanocrystals can either be used directly, with the intrinsic transitions of the nanocrystals being responsible for photon generation, or indirectly, where nanocrystals enable emission from other radiant centres through energy transfer or sensitization. For the direct approach, excitonic or defect-related emission is commonly used. Excitonic emission offers the advantage of size-related wavelength tunability, but suffers from the low efficiency of phonon-assisted recombination; devices based on this emission channel remain a challenge. An additional issue is Auger de-excitation, which, however, can be mitigated by sequential electron and hole injection. Such sequential injection may be realized in a metal–oxide–semiconductor field-effect transistor (MOSFET) structure, with the Si nanocrystals being placed as a floating gate, and electrons and holes being sequentially injected by tunnelling through a thin oxide layer (Fig. 1a,b), using an a.c. voltage of typically 10 kHz (ref. 27). Indeed, luminescence is lower at lower frequency because there are only a few recombination events per unit time, but luminescence decreases again at higher frequencies because sequential injection occurs more rapidly than the radiative lifetime in silicon nanocrystals. Defect-mediated emission

Box 2 | Properties of Si nanostructures.

Because of quantum confinement, the energy structure in a nanoconfiguration (an example for a high-resolution transmission electron microscopy image is shown in **a**) is influenced directly by the size of the nano-object, and accordingly can be 'tuned' almost at will. Additional possibilities are provided by the surface: as the surface-to-volume ratio increases with size reduction, the local arrangement of atoms located on the surface plays an increasingly important role. The combination of both effects has a profound impact on the band structure of the material and modifies both the energy and momentum dependence. Therefore, the optical bandgap and the band-to-band recombination rates can both be influenced, to the extent that an indirect-to-direct bandgap transformation can be approached. Equally, the energy bands may become discretized to such an extent that the 'band' concept ceases to apply and a molecular approach becomes more appropriate.

The energy structure of Si nanocrystals and nanowires has been thoroughly investigated experimentally, looking both at individual structures and at ensembles. It has also been extensively modelled[160–162] and good agreement with experimental data has been obtained. Regarding the optical bandgap, tuning over a wide range of energies — from about 0.9 eV in the infrared for co-doped Si nanocrystals[163] to above 4 eV in the ultraviolet for the smallest synthesized materials[164] — has been demonstrated, with up to five orders of magnitude enhancement of radiative rates compared with bulk Si (see the blueshift with decreasing size in **b** between 700 and 1,000 nm). Surface termination and strain have been explicitly shown to produce several prominent effects. In single isolated Si nanocrystals, emission spectra show phonon replicas[165–167]. In oxidized Si nanocrystals, the bandgap tunability is limited as a result of the formation of new energy levels inside the bandgap, stabilizing the photon emission energy as the nanocrystal size reduces[24]. Finally, C-capped Si nanocrystals show an interesting radiative recombination in the nanosecond range[49], as opposed to typical values in the microsecond range. Silicon nanocrystals can also be doped with shallow impurities such as B or P (ref. 168), and in the case of co-doping, the compensated nanocrystals are preferrentially formed[169]. In such materials, emission due to donor–acceptor pair recombination is observed, also with energies below the bandgap of bulk Si (refs 163,170).

Moreover, detailed investigations have revealed other effects, such as downshift of 'direct-bandgap' (see the redshift with decreasing size in panel b between 400 and 600 nm) and retardation of hot-carrier relaxation rate upon size reduction[38], the latter arising because of a combination of the lower density of states and the so-called energy 'recycling'[100,171] which provides hot carriers by Auger recombination of excitons localized in the same nanocrystal.

Figures reproduced with permission from: **a**, ref. 26, © 2003 APS; **b**, ref. 38, © 2010 NPG.

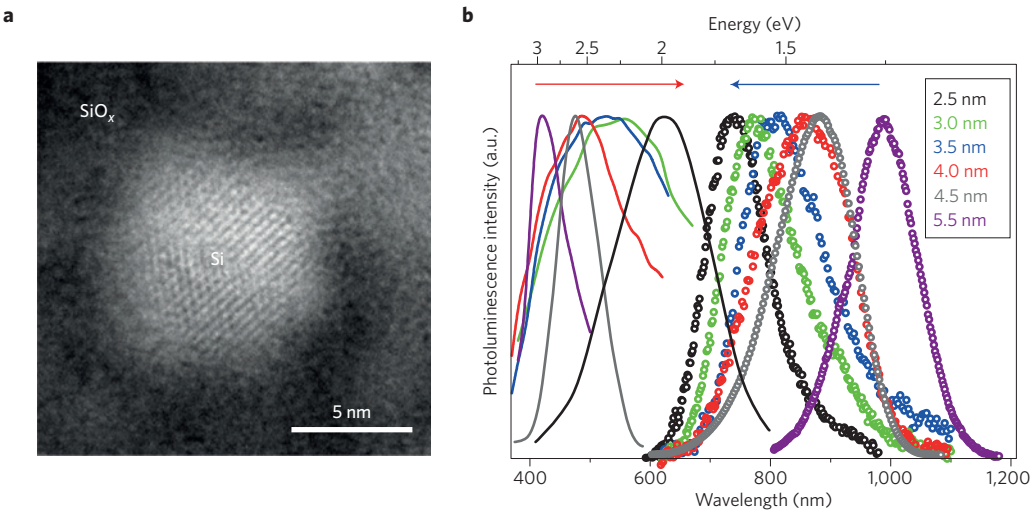

(oxygen or carbon-related) has proved to be more successful, and devices with higher efficiencies have been reported[28]. All of these devices are typically MOS-like structures with the oxide replaced by a nanocrystal-rich insulator (oxide or nitride)[29,30] (Fig. 1c). Alternatively, light-emitting devices with efficiencies of a few per cent have been fabricated with nanocrystal–organic hybrids[31]. We note, however, that so far no light-emitting devices based on Si nanocrystals have reached the market. Equally, a Si nanocrystal-based laser, despite initial successful observations of gain[32–37], has not yet been developed. One plausible yet less explored route for light emission is hot-carrier recombination, where the advantage of nanocrystals is the mitigation of phonon scattering under quantum confinement conditions. Such reduced phonon scattering slows down hot-carrier cooling, thereby enabling light emission by the phononless recombination of hot carriers, whose quantum yield increases by up to three orders of magnitude when compared with bulk Si (from 10^{-7} to 10^{-4})[38].

Although many interesting approaches for emission from direct transitions have been explored, success has been limited. The indirect approach looks more promising, especially with nanocrystals serving as sensitizers for rare-earth-doped insulating (SiO_2) or semi-insulating (Si-rich silicon oxides or nitrides) matrices. Here, the most popular system is that of Er^{3+} ions in SiO_2. Following the initial observation that Er^{3+} ions can be indirectly excited through photon absorption by Si nanocrystals[39–41], practical devices with efficiencies above the per cent level have now been demonstrated[30,42–45]. Despite this encouraging performance, only a minor fraction of all Er dopants are excited, owing to the statistical distribution of Er^{3+} ions and nanocrystals[46,47], thus precluding population inversion and laser action.

A possible breakthrough to resolve this low excitation fraction could come from surface and/or strain engineering. For example, a considerable modification of the wavefunction for the low-energy electron states can be achieved by terminating colloidal nanocrystals with carbon. This termination changes the energy structure

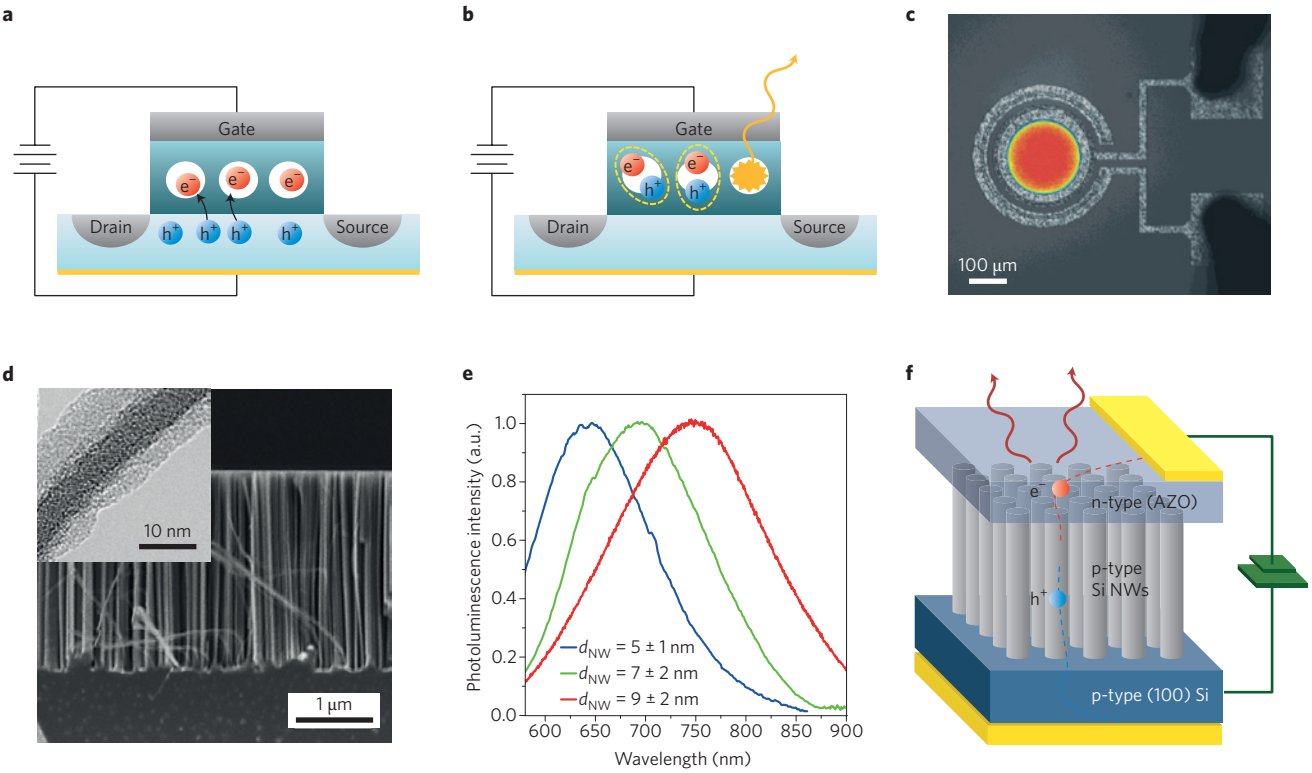

Figure 1 | Electrically driven devices based on nanocrystals and nanowires. a,**b**, Schematic of the field-effect electroluminescence mechanism in a silicon nanocrystal floating-gate transistor structure (see ref. 27). The array of Si nanocrystals embedded in the gate oxide of the transistor can be sequentially charged with electrons by Fowler–Nordheim tunnelling, and with holes by Coulomb field-enhanced Fowler–Nordheim tunnelling (**a**) to prepare excitons that radiatively recombine (**b**). **c**, Emission microscope image of a typical Si-nanocrystal electroluminescence device showing uniform emission (red) over the whole device area. **d**, Scanning electron microscope image of silicon nanowires grown by the metal-assisted chemical-etching method (see Box 1). Inset shows a transmission electron microscope image of a typical Si nanowire with sub-10-nm diameter. **e**, Size-dependent shift of the photoluminescence by Si nanowires with different mean diameters, owing to quantum confinement effect. **f**, Schematic of an electroluminescent device using p-type Si nanowires with a transparent n-type aluminium-doped ZnO (AZO) top electrode (see ref. 62). Figures reproduced with permission from: **a**,**b**, ref. 27, © 2005 NPG; **c**, ref. 29, © 2002 Springer; **d**–**f**, ref. 62, © 2012 IOP.

of the nanocrystal and hence the probability of phononless excitonic recombination. In fact, several orders of magnitude of improvement of the photoluminescence have been observed, even up to the level comparable to III–V and II–VI quantum dots[48,49]. The prospect for optical gain looks promising, and practical devices may be realized. The challenge here is the colloidal character of the materials, which makes electrical injection even more difficult than for Si nanocrystals embedded in SiO_2.

The electrical driving problems present in nanocrystals can be solved by using nanowires to provide the quantum confinement, although there are some technological issues that need to be addressed first. Nanowires are typically grown using the vapour–liquid–solid (VLS) mechanism[50] (see Box 1), which requires high-temperature (typically >450 °C) treatments. Although this method is widely used and has led to a number of successful demonstrations, it has several drawbacks: (i) uniform doping is difficult to achieve, because the dopant needs to be included in the Si flux and is difficult to incorporate into the nanowires[51,52]; (ii) there is a critical size of about 10 nm below which nanowires cannot be grown, so further oxidation is required to make them thin enough for quantum confinement[53]; (iii) Au is incorporated within the nanowires, which introduces trap levels in the gap that enhance Shockley–Read–Hall recombination[54,55]. To circumvent these issues, nanowires have been fabricated either by using VLS with titanium silicide as a catalyst[56] or by using electron beam lithography[57,58]. In both cases a subsequent oxidation step has been used to reduce the wire size. These nanowires show room-temperature luminescence compatible with quantum confinement. Metal-assisted chemical etching (MACE)[59–62] (see Box 1) is a powerful alternative, in which a dense array of Si nanowires is formed by chemical etching at room temperature, allowing easy removal of the metal after nanowire formation. The size of the nanowires can be controlled by changing the metallic pattern (see Box 1). Alternatively, their size can be modulated by coupling the metal deposition with lithography or with nanosphere self-assembly. These methods allow metal-free ultrathin nanowires to be obtained, whose doping can be easily controlled by properly doping the starting silicon substrates. Indeed, nanowires as small as 5 nm in diameter have been produced that luminesce at room temperature and that exhibit the characteristic blueshift indicative of quantum confinement (see Fig. 1d,e)[62–64]. Nanowires are ideal for light-emitting devices, as the continuity of conduction along the wire length affords easy current flow. Indeed, electroluminescent devices[62] have already been fabricated by depositing a transparent conductor (aluminium–zinc oxide, AZO) on top of the nanowires, and room-temperature performance has been demonstrated (Fig. 1f).

Light emission in silicon nanostructures was first demonstrated with porous silicon in the 1990s[65]. Efficient devices were fabricated through a substantial international effort, and a vast literature is available (for a review and a useful source of references on porous silicon, see for example ref. 66). The stability concerns, however, were never fully solved, and the research focus shifted towards the more stable silicon nanocrystals and nanowires. One of the challenges is the current flow within the quantum-confined structures. Although only in

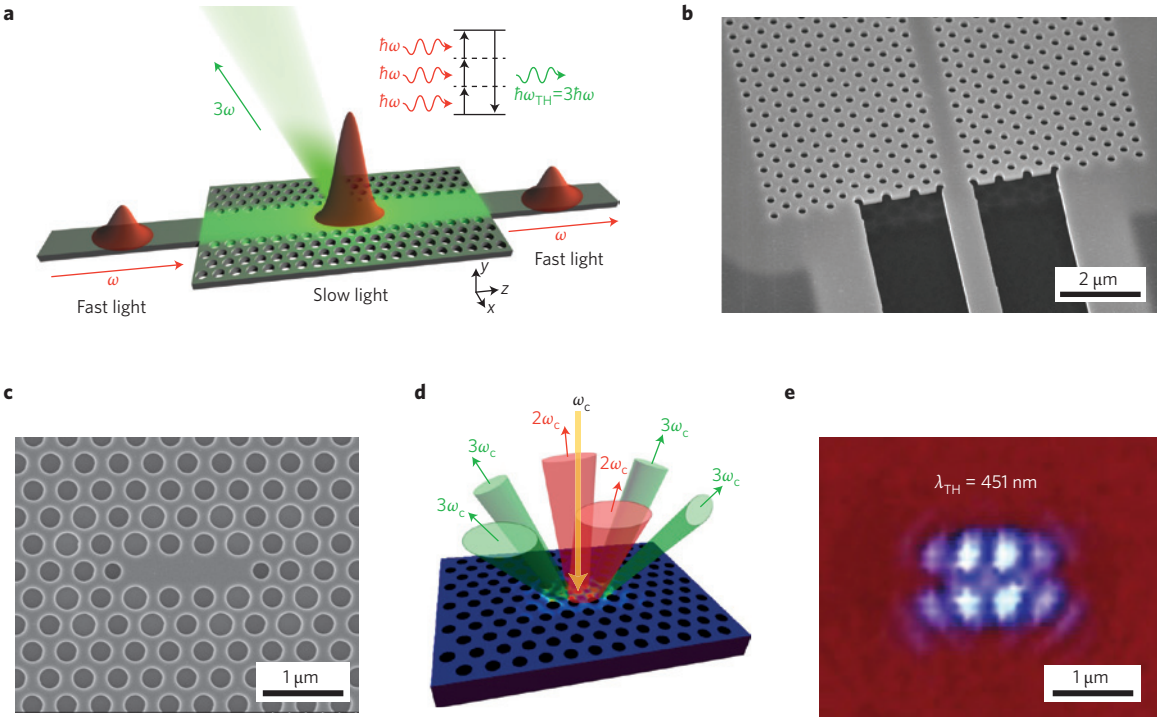

Figure 2 | Nonlinear optics in silicon photonic crystals. a, Schematic of green light emission through third-harmonic generation (THG) in a PhC waveguide operating in the slow-light regime. The fundamental pulse at frequency ω (energy $\hbar\omega$) is spatially compressed in the slow-light PhC waveguide, increasing the electric field intensity, while the third-harmonic signal, at frequency $\omega_{TH} = 3\omega$, is extracted out-of-plane by the PhC with a specific angle off the vertical direction. **b**, Scanning-electron-microscope (SEM) image of a PhC waveguide etched in a thin silicon membrane and connected to a tapered ridge waveguide. **c**, SEM image of a far-field-optimized PhC nanocavity etched in a thin silicon membrane. **d**, Schematic of the simultaneous second-harmonic (SHG) and third-harmonic generation (THG) in a far-field-optimized silicon PhC nanocavity. A low-power (mW) continuous-wave infrared laser is tuned to resonance with the fundamental cavity mode at $\omega = \omega_c$ and is vertically coupled to the PhC nanocavity from free space. Bright SHG at $\omega = 2\omega_c$ and THG at $\omega = 3\omega_c$ are emitted from the cavity to free space. **e**, Optical microscope image of the continuous-wave blue light emission from a silicon PhC nanocavity. Figures reproduced with permission from: **a**,**b**, ref. 72, © 2009 NPG; **d**, ref. 9, © 2010 OSA.

its infancy, we believe that the silicon nanowire approach offers a very promising route towards efficient silicon-based light sources.

Nanopatterning. The ability to control the flow of light with photonic crystals (PhCs)[67] has added tremendous functionality to the silicon photonic toolkit. The full benefit of PhC light confinement is derived from three-dimensional (3D) structures, but these tend to be very difficult to make and control. Instead, researchers have made impressive progress with 2D structures that rely on total internal reflection for confinement in the third dimension[68,69] (see Box 3). In fact, a key reason for the success of silicon nanotechnology in this field is that high-quality silicon-on-insulator (SOI) substrates are readily available and that fabrication is relatively simple and reliable; the best results are being achieved from electron-beam lithography with the resist (typically ZEP-520A) being directly used as a masking layer[70]. Another important feature is that some of the best results have been achieved on tools that are readily available in many laboratories; a good converted scanning electron microscope (SEM) as an electron-beam lithography tool and a basic parallel-plate reactive ion etching system may be sufficient, which is why PhC research has proliferated and many groups are engaged.

A key example for such 2D structures is the silicon line-defect PhC waveguide with engineered dispersion (see Box 3), where light can be slowed to below 1/50 of its natural speed while keeping the propagation losses low[71]. Application examples for such waveguides range from very compact and efficient delay lines to buffer memories and slow-light-enhanced nonlinear devices[72] (Fig. 2a,b). Other examples are PhC nanocavities with ultrahigh quality factors (see Box 3) that can achieve extreme light confinement in very small spaces and provide the ultimate interaction between light and matter[73–75]. For example, frequency conversion based on third-harmonic generation, which usually requires substantial pump intensity, is readily available in microscopic silicon PhC structures[9] (Fig. 2c–e); effects such as optical bistability[8], all-optical switching[76] or four-wave-mixing[77,78] have been demonstrated in silicon PhC nanostructures and are actively being researched.

Because the electromagnetic field intensity and the light–matter interaction in an optical cavity scale as its Q/V ratio, with Q the quality factor and V its modal volume, the quest for PhC nanocavities with a high Q/V ratio is intense. State-of-the-art silicon PhC cavities feature Q values in excess of 4×10^6 while keeping modal volumes below $(\lambda/n)^3$, where n is the effective index of the cavity mode[79], and performance is increasing constantly with improvements in silicon nanofabrication. The ultimate aim of the Q/V quest is to achieve single-photon nonlinearity, and this seems to be in reach[80]. This means that a single photon present in the cavity may already be sufficient to realize a nonlinear response of sufficient magnitude to detune the cavity. This would allow the realization of silicon-based single-photon sources operating at room temperature through the photon-blockade effect[81], thus taking silicon photonics further into quantum optics and quantum communications.

Although silicon photonics has almost reached maturity with respect to optical circuit elements, the light-source continues to challenge researchers, as already discussed above. Nanocavities may help to address this challenge, as they offer luminescence enhancement through the Purcell effect. The Purcell effect increases the radiative emission rate of an emitter interacting with an optical cavity by a factor proportional to the Q/V ratio; photonic

Box 3 | Fundamental properties of planar photonic crystals.

Planar photonic crystals are made by etching a periodic pattern (typically a triangular or square lattice of air holes) into a slab waveguide with high refractive index, such as Si or GaAs. In the case of Si, a silicon-on-insulator (SOI) planar waveguide is used as the starting material, and the patterned PhC membrane is released by removing the lower SiO_2 cladding with a HF-based wet etch (**a**, left panel). Typical parameters for Si PhC slabs operating at $\lambda = 1.55$ μm are a lattice constant of $a = 420$ nm, a slab thickness of $t = 220$ nm and a hole radius of $r = 130$ nm (ratio $r/a \approx 0.3$).

Planar photonic crystals are able to provide efficient optical confinement in all three dimensions by combining the 2D photonic bandgap confinement in the plane with total internal reflection (TIR) confinement in the vertical direction (**a**, right panel). In order to represent the 3D nature of the structure, the TIR confinement is superimposed on the 2D band-structure by means of the light line: only modes whose k-vectors lie below this line are guided by TIR and can propagate without losses. All other modes are subject to radiation losses and are therefore referred to as quasi-guided modes.

A line-defect waveguide is obtained by removing a single row of holes from the lattice (**b**, left panel). The dispersion curve of the waveguide arises from the interplay between photonic bandgap guiding and TIR guiding in the plane[172]; for the higher frequencies, the mode is TIR guided and the dispersion curve is relatively steep, whereas for lower frequencies, it is bandgap-guided and relatively flat (**b**, right panel). Because the group velocity is given by the slope of the dispersion curve, $v_g = d\omega/dk$, the mode is 'fast' or 'slow' depending on the operating point. Slow-light waveguides operating close to the band-edge can attain group velocities of $c/100$ or lower, but propagation becomes very lossy owing to strong back-scattering, and the dispersion becomes very high. To overcome these limitations, slow-light waveguides with 'engineered' dispersion have been introduced that allow slow-down factors of $v_g/c = 50$, relatively low loss and operation bandwidths as high as 10 nm (ref. 71). High-Q PhC nanocavities confine the light further, and they can either be understood as slow-light waveguides terminated at either end, or, more fundamentally, as intentional 'defects' introduced into the otherwise perfect photonic lattice. In analogy with solids, such defects create allowed energy states that correspond to the resonant frequencies of the cavities. The best-known examples for such point-defect cavities include the L3 nanocavity (**c**, left panel), obtained by removing three holes from the triangular lattice[72], or the heterostructure nanocavity, realized by increasing the lattice constant of a W1 waveguide, thereby creating a potential well for light[72,74]. The inventive step in both cases was the creation of a cavity mode with almost no k-vector components inside the light cone, which is achieved by a Gaussian-mode envelope. Although this insight has led to record Q-factors, now in excess of 4×10^6, being achieved, there is no useful channel available to couple light from the cavity to free space (**c**, right panel). By superimposing a secondary lattice consisting of slightly enlarged holes (**d**, left panel), we have been able to engineer the far field into a near-Gaussian output beam (**d**, right panel) while hardly compromising the cavity Q-factor[173,174]. Such far-field engineering has been instrumental for the successful observation of strongly enhanced linear and nonlinear light emission[9,88,89,92].

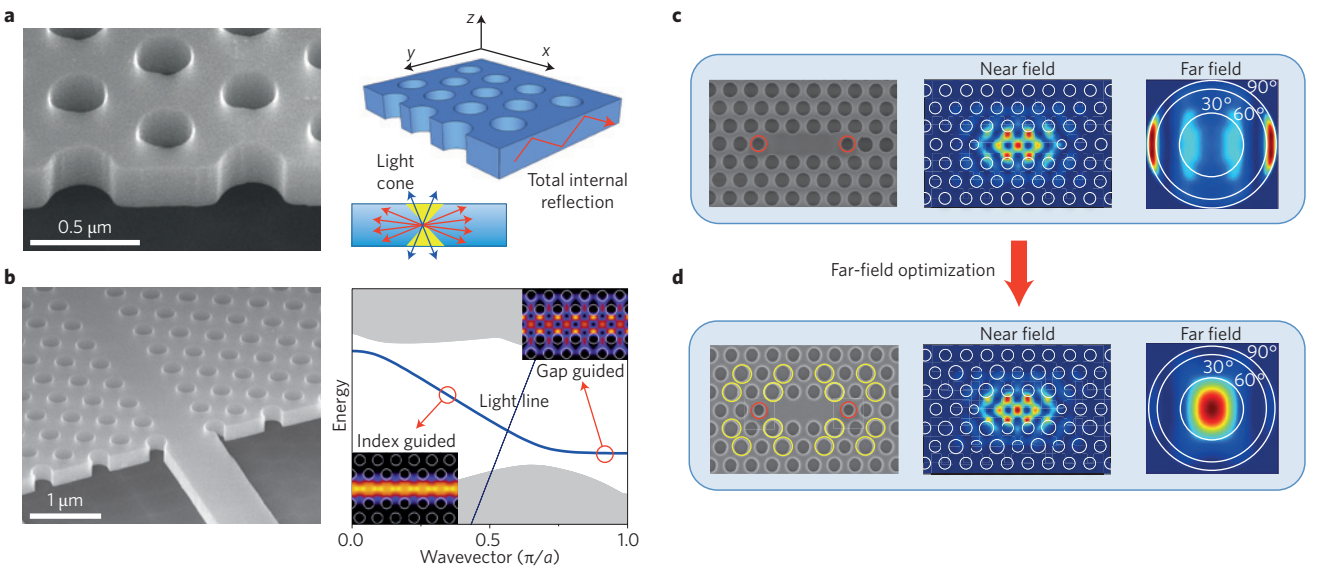

crystal cavities feature the highest Q/V ratio of any known cavity type. Indeed, enhanced emission from band-edge luminescence has already been observed with silicon PhC nanocavities resonant in the 1.1-μm range[82,83], and strong emission lines at 1.3–1.6 μm have been observed in Ge self-assembled quantum dots embedded in silicon PhC nanocavities[84,85]. Moreover, the incorporation of erbium ions in silicon nitride PhC nanocavities has enabled optically pumped transparency at 1.54 μm (refs 86,87), and recent research has shown that a thin film of erbium dioxide deposited onto a silicon nanocavity may be driven close to inversion, even at room temperature[88].

Optically active defects may also be introduced directly into silicon high-Q PhC nanocavities using a simple hydrogen plasma treatment[89]. The sub-bandgap luminescence from defects such as dislocation loops or hydrogen platelets is well studied[17,90,91], but notoriously quenches very quickly with temperature, making light-emitting devices based on these active centres impractical. Recently, the application of the Purcell effect combined with the improved extraction efficiency from a far-field-engineered PhC nanocavity (Box 3) has proved very effective in suppressing thermal quenching up to room temperature[92] and has led to an overall enhancement of light emission by more than four orders of magnitudes relative

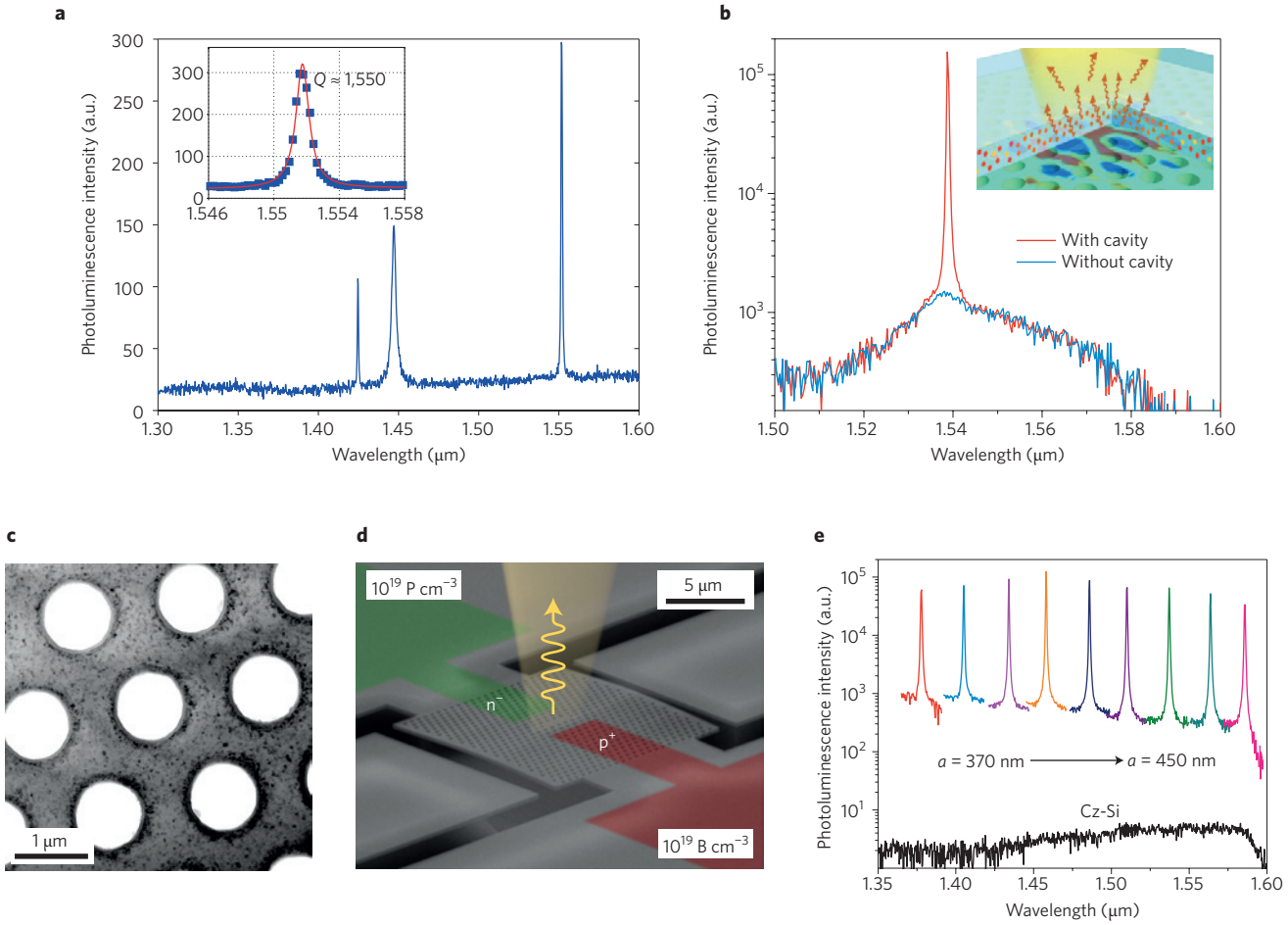

Figure 3 | Enhanced light emission from silicon photonic crystals. a, Photoluminescence spectrum of a silicon PhC nanocavity with embedded self-assembled Ge quantum dots. Enhanced emission at resonance with the cavity modes is clearly visible. **b**, Strongly enhanced light emission, by two orders of magnitude, as observed by depositing a thin (10-nm) Er_2O_3 layer on top of a silicon L3 nanocavity. The inset schematically depicts emission from a thin layer of active material interacting with the localized electromagnetic field in a PhC cavity. **c**–**e**, All-silicon photonic crystal nanocavity light-emitting diode at sub-bandgap wavelengths. A TEM image (**c**) shows the active defects (black stains) in a silicon PhC nanocavity created by hydrogen plasma treatment. **d**, SEM micrograph of a silicon photonic crystal nano-light-emitting-device. The doped regions are shown schematically and extend well into the photonic crystal. **e**, The emission line of the fundamental cavity mode of the hydrogen plasma treated cavity is four orders of magnitude higher than that of bulk Czochralski (Cz) silicon over the entire range and is tunable between 1,300 and 1,600 nm by varying the PhC lattice constant in the range a = 350–450 nm. Figures reproduced with permission from: **a**, ref. 84, © 2012 IEEE; **c**–**e**, ref. 89, © 2012 Wiley.

to bulk silicon[89] (Fig. 3). Based on this surprising result, an electrically driven nano-light-emitting-device source was also realized[89]. The device operates in a continuous-wave manner at room temperature and exhibits a narrow linewidth in the technologically important wavelength window at 1,300–1,600 nm. It is small and features low power consumption. Although it shows the highest power spectral density ever reported for a silicon light-emitting device (800 μW nm^{-1} cm^{-2}), it does not yet produce sufficient power output; otherwise, it would combine all of the desired characteristics of an integrated light source, especially given that CMOS-compatible detector technologies are also available in this wavelength range[93,94]. Nevertheless, the ability to improve the light emission properties so greatly with photonic crystal nanocavities is a very encouraging step towards the realization of all-silicon-based light sources.

Overall, a wide range of silicon-based nano-emitters have now been demonstrated, some of which show very respectable efficiency, reaching up to about 10% (refs 31,66). Even though this is impressive for an indirect-bandgap semiconductor, the brightness of such emitters is typically low and the wavelength of emission tends to be in the visible or the very near infrared (λ < 1.1 μm), where they have to compete against organic light emitters and highly efficient GaAs sources. We believe that a promising regime is the wavelength range 1.3–1.6 μm, where silicon emitters complement the extensive silicon photonics toolkit[1–11] and, combined with suitable detectors[93,94], offer the complete chain from emitter to signal-processing circuitry to detector. Furthermore, cavity-enhancement of emission is available[84,85,89,92], which can enhance efficiencies by two to three orders of magnitude[92,95]. Emitters demonstrated in this regime include those based on defects, dislocations and strain[16,17,89–91] or erbium doping[86–88], some of which have shown surprisingly high brightness[89] yet still suffer from low efficiency. The combination of nanowires and photonic crystal cavities seems particularly promising in this respect. The challenge is now to develop these concepts further as a combination of material and photonic nanostructure design in order to reach performance that can compete with integrated hybrid devices based on III–V semiconductors on silicon. Reaching such performance will signify a true breakthrough and herald the beginning of an all-silicon photonic technology.

Silicon nanostructures for photovoltaics

One of the greatest challenges facing mankind is the provision of clean energy to fuel our economies; solar cells will make an

important contribution to this challenge as part of the renewable energy mix. Of the many possible materials proposed and demonstrated for making photovoltaic solar cells, silicon is the only one that combines suitable optoelectronic properties with Earth-abundance and technological availability. Currently the highest demonstrated photovoltaic conversion efficiency of a Si solar cell is near 25%, which has been realized in a single junction configuration[96]. This is very close to the Shockley–Queisser limit of about 30% (ref. 97), and therefore only limited further progress can be expected. At the same time, Si tandems that make use of crystalline, micro/polycrystalline and amorphous forms of Si have not been able to surpass this efficiency. Consequently, the value of 25% represents the general present-day record efficiency for Si-based photovoltaics. Wafer-based 'bulk' silicon cells currently dominate the market, yet only thin-film cells will be cost-effective in the long run, as they do not require much active material and can be produced cheaply using flow-through processes on metre-sized substrates. The main trade-off of thin-film versus bulk solar cells is their reduced absorption, which introduces the need for light-trapping schemes that increase the effective absorption length of the thin-film material. Nanopatterning, quantum confinement and surface-induced effects in Si nanostructures offer interesting features that could be used to boost the efficiency of photovoltaic energy conversion and to overcome some of the restraints that lead to the Shockley–Queisser limit[98]. Specific 'photovoltaic opportunities' follow from (i) the possibility of bandgap engineering, through nanocrystals and nanowires, to modify absorption and extraction, and (ii) the possibility of new light-trapping schemes through nanopatterning.

Nanocrystals and nanowires. Silicon nanocrystals present several properties of importance for photovoltaics: (i) the possibility of tuning the bandgap and the recombination rate through quantum confinement and dedicated surface termination, (ii) the reduction of the density of states and discretization of energy levels that affect hot-carrier cooling processes, and (iii) the enhancement of the Coulomb interaction between carriers enclosed in small volumes, promoting collective effects such as multiple carrier generation (MEG)[99] and 'Auger recycling'[100]. But these advantageous properties do not arise without a price: the potential barrier that aids quantum confinement also impedes carrier extraction to the outside. In particular, this problem is notorious in all concepts of (the third-generation) solar cells based on nanocrystals. For the most readily available and most investigated system of Si nanocrystals in the solid matrix of SiO_2, the relevant potential barrier for free electrons is around 3 eV. Therefore, extraction of photogenerated carriers has to invoke tunnelling and percolation between closely spaced nanocrystals (forming 'quantum solids') which is not efficient. Several different approaches are under investigation, such as the fabrication of Si nanocrystal/organic hybrid solar cells[101]. Nanocrystals can be produced by plasma processing with the advantage of a scalable mass production for photovoltaic devices[101–105]. Demonstrated power conversion efficiencies are limited to a few per cent[101], because of the low carrier mobility, although progress can be expected. Indeed, the formation of defect/impurity-related minibands linking individual nanocrystals[106], or dispersions in several conducting media (macroporous TiO_2, polymers), is also under investigation. It seems that the ultimate solution would be a highly conductive medium with only a minimal conduction-band offset; some investigations suggest that a potential barrier as small as 0.1 eV would be sufficient to preserve advantages of quantum confinement while minimizing extraction loss. Nevertheless, the efficient extraction of free carriers from a confined environment remains a challenge.

An interesting solution to this problem may again be offered by Si nanowires. In analogy with the light-emission discussion, quantum confinement takes place in two dimensions, whereas carriers can be extracted along the third. Silicon nanowire solar cells have already been fabricated both on a single wire[107,108] and on nanowire arrays[109]. Two main schemes are used[110]: axial junctions[111,112], in which the p–i–n diode is fabricated along the length of the nanowire by varying the doping density during growth; and radial junctions[113], in which the diode is fabricated coaxially by a core–shell method. The advantages of using silicon nanowires for solar cells are multifold. First of all, nanowire arrays are extremely strong absorbers[109,114], as the light remains trapped inside the nanowire forest by multiple scattering events. Second, radial junctions have the advantage of a very short electrical path-length for carrier extraction, which would suggest the potential for significant performance improvements. In fact, efficiency depends on a compromise between the extracted current (increasing with decreasing nanowire radius) and open-circuit voltage (decreasing with increasing junction area, and hence with decreasing nanowire radius). Optimal radial junctions have a radius similar to the minority-carrier diffusion length to allow full collection without decreasing the voltage too much. A challenge is then to achieve the required high doping density needed to avoid depletion with decreasing nanowire size. In principle, quantum confinement could also be used to build cells in which the nanowires form the top part of a cell, which is transparent to less energetic photons that are absorbed at the bottom.

Both VLS growth and the MACE method have been used successfully to obtain nanowire solar cells[60,112,115]. In a nanowire solar cell the nanowire 'carpet' can be conformally covered by a transparent electrode such as AZO embedded within a conductive polymer or alternatively infiltrated by a liquid electrode. The resulting solar cells have all the advantages of a highly absorbing material with a radial, low-path, carrier extraction. One might expect that the better performance is obtained by maximizing carrier extraction and hence carrier lifetime, which is, indeed, achieved by minimizing trap centres. This is in principle easier with the MACE method, as the preparation is at room temperature and the detrimental effect of metal diffusion does not occur. In fact solar cells with efficiencies over 10% have already been claimed[116], with further progress being expected.

Silicon nanostructures not only allow us to make traditional 'photon-in/electron-out' photovoltaic devices; they can also form the basis of an autonomous device — a 'solar shaper'. Such a photon-in/photon-out scheme does not involve carrier extraction, but it would be used to extract energy from the parts of the solar spectrum that are otherwise not efficiently converted. It therefore rectifies the fundamental reason for the limited efficiency of photovoltaic conversion: the mismatch between the broadband character of solar radiation and the narrow window of optimal performance of a semiconductor photodiode. A solar 'shaper' could form an add-on that supplements the traditional cell and converts the incoming broadband spectrum into a new spectrum that is narrower and better optimized for absorption by a single-junction solar cell. This would require the 'cutting' of high-energy ultraviolet photons into multiple lower-energy quanta that can be converted more efficiently, as well as the 'pasting' together of low-energy photons in the near infrared that are otherwise not converted at all. Silicon nanocrystals offer interesting possibilities that could be used for both processes.

For photon cutting, the MEG process mentioned previously could be used (Fig. 4a). In this process, a highly energetic hot carrier relaxes by generating additional electron–hole pairs. MEG is usually seen as a direct analogue of impact excitation in bulk materials, whose efficiency in nanocrystals is enhanced by a high density of carriers in a strongly confined environment. The effect was first reported in nanocrystals of direct-bandgap materials[117] and later also in (colloidal) Si (ref. 118). Dedicated investigations confirmed that the efficiency of this process in nanocrystals is considerably enhanced when compared with bulk materials of the same bandgap[119,120]. Applied to photovoltaics, MEG would create more than

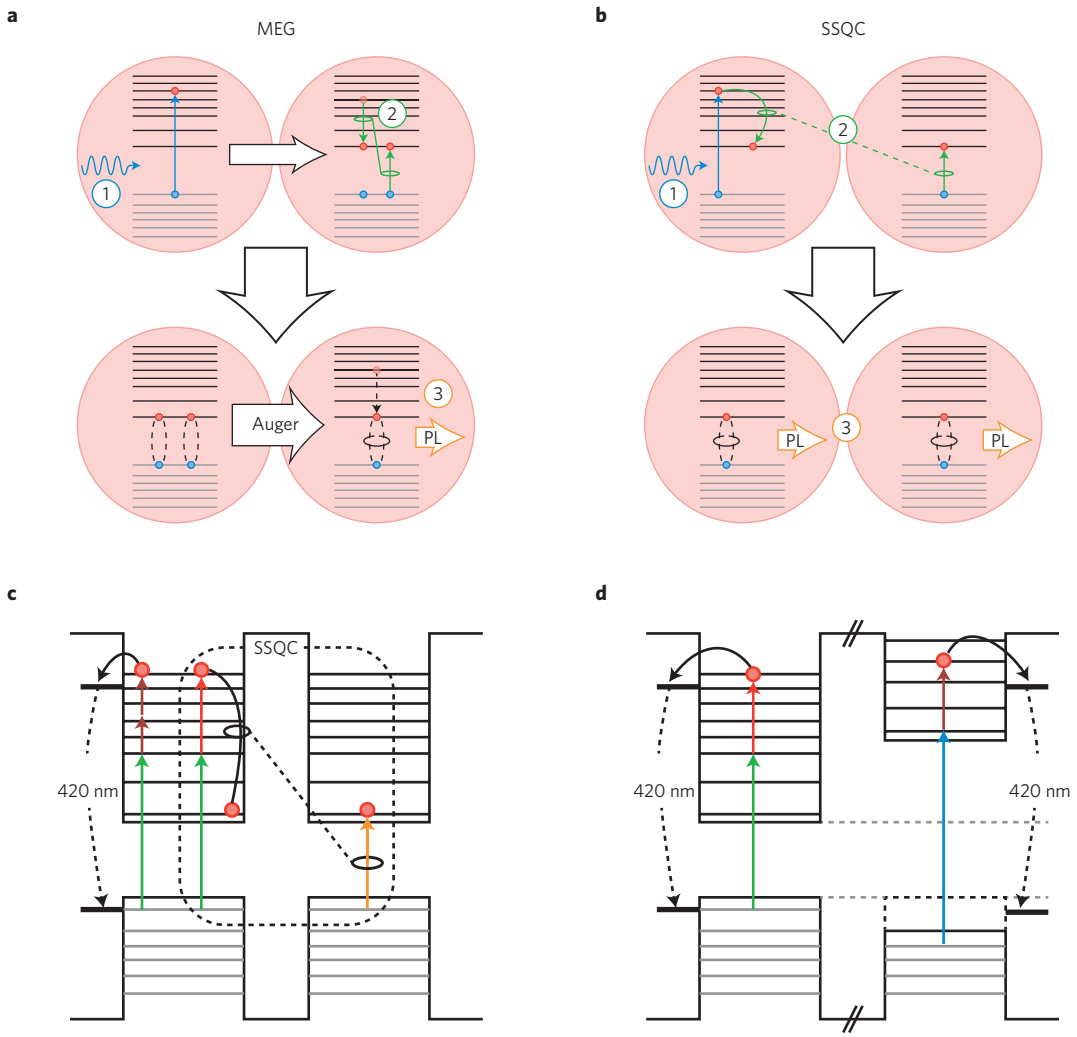

Figure 4 | Photon cutting and pasting by Si nanocrystals. a,**b**, Photon cutting. **a**, In MEG a hot carrier is created on absorption of a high-energy photon (1), and then cools down by generating a second exciton (2). Efficient Auger interaction allows for photoluminescence (PL) from only one exciton (3). **b**, In space-separated quantum cutting (SSQC), the excess energy of the hot carrier is used to generate an exciton in a neighbouring (coupled) nanocrystal. The separated excitons are now both able to recombine radiatively. **c**,**d**, Photon pasting. **c**, Absorption of low-energy (below-bandgap) photons by free carriers (generated by photons with $E_{exc} > E_{gap}$). The resulting hot carrier can be trapped at a surface-related defect level (420 nm) or undergo spatially separated multiplication. **d**, Nanocrystals with different bandgap sizes (but with the fixed 420-nm line) can be used to absorb and trap infrared photons of different energy. By tuning the nanocrystal diameter, absorption for specific infrared photons can be optimized.

one electron–hole pair per single absorbed high-energy photon, thereby creating additional photocurrent from the green and blue part of the solar spectrum. Indeed, theoretical evaluations indicate that total conversion efficiencies of up to ~50% are feasible — that is, efficiencies well above the Shockley–Queisser limit[121]. The lifetime of the multiple carriers generated in this process is limited by their Auger interaction and depends on the nanocrystal size and carrier multiplicity, but generally remains in the subnanosecond range[121,122], which is too short. For dense solid-state dispersions of Si nanocrystals in SiO_2 (ref. 123), however, multiple excitons that are generated on absorption of a single high-energy photon can appear not in the same but in neighbouring nanocrystals[100]; this spatial separation reduces Auger interaction, allowing for radiative recombination of multiple excitons and the emission of several photons of lower energy. Detailed investigations[124,125] showed that this process of space-separated quantum cutting (Fig. 4b) can be very efficient, doubling the number of emitted photons for energies as low as 0.3 eV above the energy conservation limit (of $2E_{gap}$). Therefore the photon cutting effect could also open new opportunities for eventual schemes of carrier extraction, because in 'multiplied' carriers the lifetime is increased from the typical subnanosecond range to tens or even hundreds of microseconds.

Recent investigations revealed that Si nanocrystals may also be suitable for photon pasting. The most important properties in this respect are (i) the identification of phononless recombination[38], (ii) a significant reduction of the cooling rate for hot carriers, (iii) a large cross-section of free carriers for the absorption of infrared photons, and (iv) defect-related hot-carrier photoluminescence. These properties, especially in combination, open perspectives for photovoltaic conversion of infrared photons that are otherwise lost. Two specific approaches that make use of such combined effects are currently under investigation (see Fig. 4). The first is the absorption of low-energy photons by free carriers for the generation of hot excitons, followed by carrier multiplication, shown in Fig. 4c, or trapping at the Si–O related defect and subsequent 'blue' emission at ~420 nm (refs 126,127). We point out that because the 420-nm wavelength of the hot defect-related emission is fixed, the absorption of the infrared photons can be tailored by changing the nanocrystal size, as highlighted in Fig. 4d. A second approach makes use of the nonlinear properties of Si nanocrystals, more specifically the combined

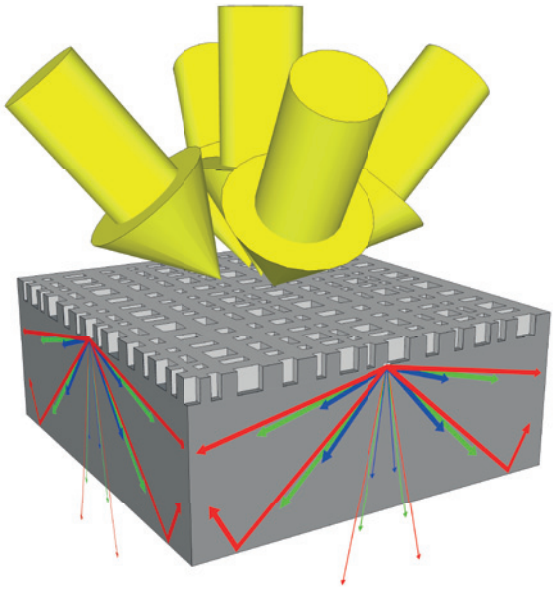

Figure 5 | Supercell binary grating for light trapping. The supercell geometry provides all of the necessary degrees of freedom to maximize light trapping, while being easy to fabricate. The figure highlights the structure's ability to excite the quasi-guided modes of the thin film while diverting the diffracted energy away from the orders that transmit in a single pass.

absorption of two (or more) low-energy photons for the generation of a single low-energy electron–hole pair[128].

In general, in addition to these opportunities and unique properties, Si nanostructures offer one key advantage over other approaches for next-generation photovoltaics, namely the use of Si itself. Silicon nanostructures add the important degrees of freedom of bandstructure engineering and surface modification to the abundance, minimal environmental footprint and technological maturity of the Si material.

Light trapping. The main trade-off of thin-film versus bulk solar cells is their reduced absorption, which introduces the need for light-trapping schemes that increase the effective absorption length of the thin-film material. Nanophotonic techniques are particularly promising for the purpose of light trapping, as they allow us to control the flow of light on the length scale of several 100 nm to a few micrometres that is required for thin-film solar cells. Researchers are pursuing two different paradigms, plasmonic and diffractive light trapping; here, we focus on diffractive effects, as we believe that the inevitable absorption incurred by plasmonic nanostructures makes it even more challenging to achieve the desired high efficiencies, and to convert every incoming photon into an electron–hole pair (for a recent review on plasmonics for photovoltaic devices see ref. 129).

The key figure of merit for any light-trapping scheme is the Lambertian limit[130,131], which has a maximum value of $4n^2$ and is a measure for the achievable pathlength compared with a single pass through the material; a photon may travel up to $4n^2$ times further than without light trapping, and hence increase its chances of being absorbed. The $4n^2$ limit assumes very weak absorption, and only applies if the path-length is much smaller than the absorption length; for thicker or more strongly absorbing materials, it is correspondingly smaller. For example, for a 100-nm-thick crystalline silicon film, light trapping close to the Lambertian limit may be achieved, whereas a factor of 2 is the most that can be expected for an amorphous Si (a-Si) film of the same thickness[132]. An additional effect of nanostructures is their ability to completely suppress back-reflections, which has led to the term 'black silicon'[133–135] being used to describe this property.

What type of structure to use in order to achieve light trapping in a thin-film solar cell is a question that is actively being researched, with the options ranging from random surface roughness, which excites many diffraction orders, to ordered gratings that only excite a few. Recent trends indicate that the optimum light-trapping structure lies somewhere in-between; the diffraction orders generated by random scattering are too weak, but there are not enough of them created by regular ordered gratings. Furthermore, neither extreme provides sufficient degrees of freedom to account for the wavelength-dependent absorption of the active layer. Accordingly, a number of structures that have been developed using numerical optimization techniques appear quasi-random[136] or periodic with a more complex unit cell[137,138]. Similarly, structures making use of multiple light scattering and wave interference in two-dimensional random media have shown increased light-trapping properties[139], as have periodic structures that were partially randomized[140] and randomly rough structures with Gaussian disorder[141]. Structures with more complex three-dimensional unit cells are also being investigated and have shown light-trapping performance close to the Lambertian limit[142,143], but they are more challenging to fabricate, especially on the large scales required for cost-effective mass-production. The consideration of mass-manufacturability adds an important boundary condition, namely that of simplicity, which drives the search for structures such as binary gratings that are intrinsically easy to make yet still high-performing[137,144] (see Fig. 5).

Ultimately, researchers aim to surpass the Lambertian limit, especially as this limit was derived for thick-film cells and relies on geometric optics, whereas for thin-film cells, wave optics rules. Proposals for new structures that may surpass this limit in the wave-optics regime and for a limited wavelength range have already been made[145], but an experimental structure that surpasses the Lambertian limit for all angles and in the full wavelength region of interest remains elusive and poses an exciting research challenge for the future.

Another challenge is to use light-trapping techniques without compromising the electro-optic properties of the material. For example, etching a nanostructure into silicon greatly increases the surface recombination velocity, with values up to 10^5 cm s^{-1} having been reported[146], which severely degrades the photovoltaic efficiency. A possible solution to this issue may be a thin film deposited by atomic layer deposition, which has shown promising improvements[147] or the careful control of the surface doping profile[133], which can be used to limit both surface and Auger recombination. Alternatively, the active silicon film may be deposited onto a pre-patterned substrate, but then the material properties of the film may also be compromised[148,149].

To summarize, silicon, owing to its Earth-abundance and near-optimum electronic bandgap, is the prime candidate for realizing large-scale photovoltaic systems. Reducing the amount of material while maintaining high efficiencies is the key research goal in order to drive cost reduction. A number of silicon nanostructures have now been demonstrated for enhancing performance, for example by multiplying carriers through 'photon cutting' (MEG)[117–125], by reducing reflections (black silicon)[133–135], by maximizing absorption through careful bandgap engineering (quantum dots and nanowires) or through light trapping in thin films[135–140].

Designs based on random, amorphous and periodic (including 'quasi-random' periodic) nanostructures have been proposed, with very promising performance being predicted. The figure of merit that is emerging to describe such light-trapping nanostructures is how close the performance of the nanostructure comes to the ideal scattering (Lambertian) limit. Using advanced designs, the performance may even be extended beyond that of a Lambertian scatterer by taking wave-optics effects into account[145]. Objective comparisons of the different types of structure discussed in the literature are difficult, however, as the maximum enhancement achievable with a given nanostructure depends on the nature of the material

(for example, a-Si versus c-Si or III–V) and its thickness; how the nanostructure affects the electro-optic performance of the solar cell, for example through parasitic absorption in the contacts, or through surface and Auger recombination, is another important issue, as well as the question of whether the overall performance of a solar cell can be enhanced using 'solar shapers' that convert the spectrum in order to optimize electron–hole pair generation. Given the intense pressure on the cost-effectiveness of solar cells, the key challenge is to design nanostructures that enhance the electro-optic performance of the cell while being manufacturable at large scale and at sufficiently low cost.

Challenges and perspectives

Silicon, as a monoatomic crystal, offers only very limited degrees of freedom for manipulating its optoelectronic properties. It is therefore impressive how many methods, mainly based on nanoscale engineering, have been developed to extend its capabilities. These methods either manipulate silicon's intrinsic electronic properties using quantum size and surface effects or they add photonic functionality through wavelength-scale nanostructures such as photonic crystals. We have provided an overview of the most promising of these methods and have outlined the outstanding challenges.

Silicon nanocrystals, without doubt, have been one of the most important developments in the field, as they offer strong carrier confinement and modification of the energy levels through quantization, as well as the ability to use their surface as a further design parameter. This has now led to the truly remarkable observation of photoluminescence levels from these nanocrystals that are comparable to those of direct-bandgap quantum dots. Electroluminescence remains a challenge, however, because the dielectric matrix (typically SiO_2) makes it difficult to inject and extract carriers. Silicon nanowires offer an interesting alternative, as they combine strong confinement with a readily available conduction path. Such nanowires are still in their early stages of development, however, with the main challenge being the development of a reliable and impurity-free growth method. Once this has been achieved, we can look forward to silicon nanostructures combining quantum-dot-like optical properties and with electrical conduction that may ultimately rival III–V materials.

An alternative to the bottom-up creation of nanocrystals and wires is the top-down incorporation of photoactive defects into the silicon matrix. Many studies on such defects have been performed, but surprisingly little is known about their light-emission properties. Recent studies linking these defects to strong luminescence have revitalized the interest, especially following the remarkable demonstration of light emission of similar strength to that from comparable III–V photonic crystal cavities. If one could better control the nature of the photoactive defects and increase their density, thereby increasing the spectral density of emission, a true all-silicon laser might well be in reach.

Regarding wavelength-scale photonic nanostructures, photonic crystals have clearly proved their value as part of the silicon photonics toolkit; in addition to enabling some of the smallest and lowest-power modulators for communications applications, they offer the highest Purcell enhancement of any known resonant system and are therefore essential for any application involving radiative transitions. The main issue is that the surface damage incurred during their fabrication leads to high surface recombination velocities, which is detrimental to both light emitters and solar cells. Recent demonstrations involving atomic layer deposition have shown, however, that the surface damage can be mitigated to a considerable extent.

Silicon nanostructures have mainly been developed with light emission and propagation in mind, but many concepts can readily be applied to the complementary problem of light absorption in solar cells. Arguably, silicon is the only viable material for the large-scale production of solar cells, owing to its abundance and technological maturity, so improving its light-trapping properties is a worthwhile pursuit. Correspondingly, a number of authors have now proposed solutions that can reach the Lambertian limit of maximum absorption enhancement in thin-film solar cells. The main challenge is to implement light-trapping designs in electrically viable material and to ensure that the designs can be realized on the required large areas ('nanostructures on square metres') in a cost-effective manner. From the design perspective, an exciting question is whether the Lambertian limit can be beaten across the relevant solar spectrum, which would provide a further boost to solar-cell efficiency.

Given the large market pull for photonic technologies and the many innovative solutions provided by industrial and academic research groups, there is no doubt that Si photonics will mature further and will evolve to become the dominant technology also in photonics. We hope that our Review will contribute to this development and that it will provide inspiration for even better solutions.

Received 26 July 2013; accepted 12 November 2013; published online 6 January 2014

References

1. Claps, R. *et al.* Observation of stimulated Raman scattering in silicon waveguides. *Opt. Express* **11,** 1731–1739 (2003).
2. Rong, H. *et al.* An all-silicon Raman laser. *Nature* **433,** 725–728 (2005).
3. Rong, H. *et al.* Low-threshold continuous-wave Raman silicon laser. *Nature Photon.* **1,** 232–237 (2007).
4. Takahashi, Y. *et al.* A micrometre-scale Raman silicon laser with a microwatt threshold. *Nature* **498,** 470–474 (2013).
5. Liu, A. *et al.* A high-speed silicon optical modulator based on a metal–oxide–semiconductor capacitor. *Nature* **427,** 615–618 (2004).
6. Reed, G. T., Mashanovich, G. Z., Gardes, F. Y. & Thomson, D. J. Silicon optical modulators. *Nature Photon.* **4,** 518–526 (2010).
7. Miller, D. A. B. Device requirements for optical interconnects to silicon chips. *Proc. IEEE* **97,** 1166 (2009).
8. Notomi, M. *et al.* Optical bistable switching action of Si high-*Q* photonic-crystal nanocavities. *Opt. Express* **13,** 2678–2687 (2005).
9. Galli, M. *et al.* Low-power continuous-wave harmonic generation in silicon photonic crystal cavities. *Opt. Express* **18,** 26613–26624 (2010).
10. Matsuo, S. *et al.* 20-Gbit/s directly modulated photonic crystal nanocavity laser with ultra-low power consumption. *Opt. Express* **19,** 2242–2250 (2011).
11. Debnath, K. *et al.* Cascaded modulator architecture for WDM applications. *Opt. Express* **20,** 27420–27428 (2012).
12. Fujita, M., Takahashi, S., Tanaka, Y., Asano, T. & Noda, S. Simultaneous inhibition and redistribution of spontaneous light emission in photonic crystals. *Science* **308,** 1296–1298 (2005).
13. Weber, J. & Alonso, M. I. Near-band-gap photoluminescence of Si–Ge alloys. *Phys. Rev. B* **40,** 5683–5693 (1989).
14. Kenyon, A. J. Erbium in silicon. *Semicond. Sci. Technol.* **20,** R65–R84 (2005).
15. Vinh, N. Q., Ha, N. N. & Gregorkiewicz, T. Photonic properties of Er-doped crystalline silicon. *Proc. IEEE* **97,** Spec. Issue (7) on Silicon Photonics, 1269–1283 (2009).
16. Ng, W. L. *et al.* An efficient room-temperature silicon-based light-emitting diode. *Nature* **410,** 192–194 (2001).
17. Cloutier, S. G., Kossyrev, P. A. & Xu, J. Optical gain and stimulated emission in periodic nanopatterned crystalline silicon. *Nature Mater.* **4,** 887–891 (2005).
18. Ossicini, S., Pavesi, L. & Priolo, F. *Light Emitting Silicon for Microphotonics* (Springer, 2004).
19. Shirasaki, Y., Supran, G. J., Bawendi, M. G. & Bulović, V. Emergence of colloidal quantum-dot light-emitting technologies. *Nature Photon.* **7,** 13–23 (2013).
20. Talapin, D. V., Lee, J. S., Kovalenko, M. V. & Shevchenko, E. V. Prospects of colloidal nanocrystals for electronic and optoelectronic applications. *Chem. Rev.* **110,** 389–458 (2010).
21. Pavesi, L. & Turan, R. (eds) *Silicon Nanocrystals; Fundamentals, Synthesis, and Applications* (Wiley-VCH, 2010).
22. Koshida, N. (ed.) *Nanostructure Science and Technology: Device Applications of Silicon Nanocrystals and Nanostructures* (Springer, 2008).
23. Sykora, M. *et al.* Size-dependent intrinsic radiative decay rates of silicon nanocrystals at large confinement energies. *Phys. Rev. Lett.* **100,** 067401 (2008).
24. Wolkin, M., Jorne, J., Fauchet, P., Allan, G. & Delerue, C. Electronic states and luminescence in porous silicon quantum dots: the role of oxygen. *Phys. Rev. Lett.* **82,** 197–200 (1999).

25. Godefroo, S. *et al.* Classification and control of the origin of photoluminescence from Si nanocrystals. *Nature Nanotech.* **3,** 174–178 (2008).
26. Daldosso, N. *et al.* Role of the interface region on the optoelectronic properties of silicon nanocrystals embedded in SiO_2. *Phys. Rev. B* **68,** 085327 (2003).
27. Walters, R. J., Bourianoff, G. I. & Atwater, H. A. Field-effect electroluminescence in silicon nanocrystals. *Nature Mater.* **4,** 143–146 (2005).
28. Dohnalova, K. *et al.* White-emitting oxidized silicon nanocrystals: Discontinuity in spectral development with reducing size. *J. Appl. Phys.* **107,** 053102 (2010).
29. Franzò, G. *et al.* Electroluminescence in silicon nanocrystal MOS structures. *Appl. Phys. A* **74,** 1–5 (2002).
30. Yerci, S., Li, R. & Dal Negro L. Electroluminescence from Er-doped Si-rich silicon nitride light emitting diodes. *Appl. Phys. Lett.* **97,** 081109 (2010).
31. Cheng, K-Y., Anthony, R., Kortshagen, U. R. & Holmes, R. J. High-efficiency silicon nanocrystal light-emitting devices. *Nano Lett.* **11,** 1952–1956 (2011).
32. Pavesi, L., Dal Negro, L., Mazzoleni, L., Franzo, G. & Priolo, F. Optical gain in silicon nanocrystals. *Nature* **408,** 440–444 (2000).
33. Dohnalova, K. *et al.* Optical gain at the F-band of oxidized silicon nanocrystals. *J. Phys. D* **42,** 135102 (2009).
34. Khriachtchev, L., Rasanen, M., Novikov, S. & Sinkkonen, J. Optical gain in Si/SiO_2 lattice: experimental evidence with nanosecond pulses. *Appl. Phys. Lett.* **79,** 1249–1252 (2001).
35. Ruan, J., Fauchet, P. M., Dal Negro, L., Cazzanelli, M. & Pavesi, L. Stimulated emission in nanocrystalline silicon superlattices. *Appl. Phys. Lett.* **83,** 5479–5482 (2003).
36. Dal Negro, L. *et al.* Dynamics of stimulated emission in silicon nanocrystals *Appl. Phys. Lett.* **82,** 4636–4639 (2003).
37. Luterova, K. *et al.* Optical gain in porous silicon grains embedded in sol–gel derived SiO_2 matrix under femtosecond excitation. *Appl. Phys. Lett.* **8,** 3280–3283 (2004).
38. De Boer, W. D. A. M. *et al.* Red spectral shift and enhanced quantum efficiency in phonon-free photoluminescence from silicon nanocrystals. *Nature Nanotech.* **5,** 878–884 (2010).
39. Kenyon, A. J., Trwoga, P. F., Federighi, M. & Pitt, C. W. Optical properties of PECVD erbium-doped silicon-rich silica: evidence for energy transfer between silicon microclusters and erbium ions. *J. Phys. Condens. Matter* **6**, L319 (1994).
40. Fujii, M., Yoshida, M., Kanzawa, Y., Hayashi, S. & Yamamoto, K. 1.54 μm photoluminescence of Er^{3+} doped into SiO_2 films containing Si nanocrystals: Evidence for energy transfer from Si nanocrystals to Er^{3+}. *Appl. Phys. Lett.* **71,** 1198–1201 (1997).
41. Priolo, F., Franzò, G., Iacona, F., Pacifici, D. & Vinciguerra, D. Role of energy transfer on the optical properties of undoped and Er-doped interacting silicon nanocrystals. *J. Appl. Phys.* **89,** 264 (2001).
42. Iacona, F. *et al.* Electroluminescence at 1.54 μm in Er-doped Si nanocluster-based devices. *Appl. Phys. Lett.* **81,** 3242 (2002).
43. Irrera, A. *et al.* Influence of the matrix properties on the performances of Er-doped Si nanoclusters light emitting devices. *J. Appl. Phys.* **107,** 054302 (2010).
44. Ramirez, J. M. *et al.* Erbium emission in MOS light emitting devices: from energy transfer to direct impact excitation. *Nanotechnology* **23,** 125203 (2012).
45. Tengattini, A. *et al.* Toward a 1.54 μm electrically driven erbium-doped silicon slot waveguide and optical amplifier. *J. Lightwave Technol.* **31,** 391–397 (2013).
46. Wojdak, M. *et al.* Sensitization of Er luminescence by Si nanoclusters. *Phys. Rev. B* **69,** 233315 (2004).
47. Izeddin, I. *et al.* Energy transfer processes in Er-doped SiO_2 sensitized with Si nanocrystals. *Phys. Rev. B* **78,** 035327 (2008).
48. Dohnalová, K. *et al.* On microscopic origin of the fast blue-green luminescence from chemically synthesized non-oxidized silicon quantum dots. *Small* **8,** 3185–3191 (2012).
49. Dohnalova, K. *et al.* Surface brightens-up Si quantum dots: Direct bandgap-like size-tunable emission. *Light: Sci. Applic.* **2,** e47 (2013).
50. Wagner, R. S. & Ellis, W. C. Vapour–liquid–solid mechanism of single crystal growth. *Appl. Phys. Lett.* **4,** 89 (1964).
51. Koren, E., Berkovitch, N. & Rosenwaks, Y. Measurement of active dopant distribution and diffusion in individual silicon nanowires. *Nano Lett.* **10,** 1163–1167 (2010).
52. Koren, E. *et al.* Obtaining uniform dopant distributions in VLS-grown Si nanowires. *Nano Lett.* **11,** 183–187 (2011).
53. Dubrovskii, V., Sibirev, N., Harmand, J. & Glas, F. Growth kinetics and crystal structure of semiconductor nanowires. *Phys. Rev. B* **78,** 235301 (2008).
54. Bailly, A. *et al.* Direct quantification of gold along a single Si nanowire. *Nano Lett.* **8,** 3709–3714 (2008).
55. Koren, E. *et al.* Direct measurement of individual deep traps in single silicon nanowires. *Nano Lett.* **11,** 2499–2502 (2011).
56. Guichard, A. R., Barsic, D. N., Sharma, S., Kamins, T. I. & Brongersma, M. L. Tunable light emission from quantum-confined excitons in $TiSi_2$-catalyzed silicon nanowires. *Nano Lett.* **6,** 2140–2144 (2006).
57. Walavalkar, S. S. *et al.* Tunable visible and near-IR emission from sub-10 nm etched single-crystal Si nanopillars. *Nano Lett.* **10,** 4423–4428 (2010).
58. Valenta, J., Bruhn, B. & Linnros, J. Coexistence of 1D and quasi-0D photoluminescence from single silicon nanowires. *Nano Lett.* **11,** 3003–3009 (2011).
59. To, W-K., Tsang, C-H., Li, H-H. & Huang, Z. Fabrication of n-type mesoporous silicon nanowires by one-step etching. *Nano Lett.* **11,** 5252–5258 (2011).
60. Sivakov, V. *et al.* Silicon nanowire-based solar cells on glass: synthesis, optical properties, and cell parameters. *Nano Lett.* **9,** 1549–1554 (2009).
61. Huang, Z. P. *et al.* Extended arrays of vertically aligned sub-10 nm diameter [100] Si nanowires by metal-assisted chemical etching. *Nano Lett.* **8,** 3046–3051 (2008).
62. Irrera, A. *et al.* Quantum confinement and electroluminescence in ultrathin silicon nanowires fabricated by a maskless etching technique. *Nanotechnology* **23,** 075204 (2012).
63. Artoni, P. *et al.* Temperature dependence and aging effects on silicon nanowires photoluminescence. *Opt. Express* **20,** 1483–1490 (2012).
64. Pecora, F. *et al.* Nanopatterning of silicon nanowires for enhancing visible photoluminescence. *Nanoscale* **4,** 2863–2866 (2012).
65. Canham, L. T. Silicon quantum wire array fabrication by electrochemical and chemical dissolution of wafers. *Appl. Phys. Lett.* **57,** 1046–1048 (1990).
66. Bisi, O., Ossicini, S. & Pavesi, L. Porous silicon: a quantum sponge structure for silicon based optoelectronics. *Surf. Sci. Rep.* **38,** 1c126 (2000).
67. Joannopoulos, J., Johnson, S. G., Meade, R. & Winn, J. *Photonic Crystals: Molding the Flow of Light* 2nd edn (Princeton Univ. Press, 2007).
68. Krauss, T. F., De La Rue, R. M. & Brand, S. Two-dimensional photonic-bandgap structures operating at near-infrared wavelengths. *Nature* **383,** 699–702 (1996).
69. Notomi, M. Manipulating light with strongly modulated photonic crystals. *Rep. Prog. Phys.* **73,** 096501 (2010).
70. Reardon, C., Rey, I. H., Welna, K., O'Faolain, L. & Krauss, T. F. Fabrication and characterization of photonic crystal slow light waveguides and cavities. *J. Vis. Exp.* **69**, e50216 (2010).
71. O'Faolain, L. *et al.* Loss engineered slow light waveguides. *Opt. Express* **18,** 27627–27638 (2010).
72. Corcoran, B. *et al.* Green light emission in silicon through slow-light enhanced third-harmonic generation in photonic-crystal waveguides. *Nature Photon.* **3,** 206–210 (2009).
73. Akahane, Y., Asano, T., Song, B. S. & Noda, S. High-*Q* photonic nanocavity in a two-dimensional photonic crystal. *Nature* **425,** 944–947 (2004).
74. Notomi, M., Kuramochi, E. & Taniyama, H. Ultrahigh-*Q* nanocavity with 1D photonic gap. *Opt. Express* **16,** 11095–11102 (2008).
75. Song, B. S., Noda, S., Asano, T. & Akahane, Y. Ultra-high-*Q* photonic double-heterostructure nanocavity. *Nature Mater.* **4,** 207–210 (2005).
76. Tanabe, T. *et al.* Fast all-optical switching using ion-implanted silicon photonic crystal nanocavities. *Appl. Phys. Lett.* **90,** 031115 (2007).
77. Li, J., O'Faolain, L., Rey, I. H. & Krauss, T. F. Four-wave mixing in photonic crystal waveguides: slow light enhancement and limitations. *Opt. Express* **19,** 4458–4463 (2011).
78. Xiong, C. *et al.* Slow-light enhanced correlated photon pair generation in a silicon photonic crystal waveguide. *Opt. Lett.* **36,** 3413–3415 (2011).
79. Taguchi, Y., Takahashi, Y., Sato, Y., Asano, T. & Noda, S. Statistical studies of photonic heterostructure nanocavities with an average *Q* factor of three million. *Opt. Express* **19,** 11916–11921 (2011).
80. Ferretti, S. & Gerace, D. Single-photon nonlinear optics with Kerr-type nanostructured materials, *Phys. Rev. B* **85,** 033303 (2012).
81. Volz, T. *et al.* Ultrafast all-optical switching by single photons. *Nature Photon.* **6,** 607–611 (2012).
82. Iwamoto, S., Arakawa, Y. & Gomyo, A. Observation of enhanced photoluminescence from silicon photonic crystal nanocavity at room temperature. *Appl. Phys. Lett.* **91,** 211104 (2007).
83. Hauke, N. *et al.* Enhanced photoluminescence emission from two-dimensional silicon photonic crystal nanocavities. *New J. Phys.* **12,** 053005 (2010).
84. Xu, X. *et al.* Silicon-based light-emitting devices based on Ge self-assembled quantum dots embedded in optical cavities. *IEEE J. Sel. Topics Quantum Electron.* **18,** 1830 (2012).
85. Xu, X. *et al.* High-quality-factor light-emitting diodes with modified photonic crystal nanocavities including Ge self-assembled quantum dots on silicon-on-insulator substrates. *Appl. Phys. Express* **5,** 102101 (2012).
86. Gong, Y. *et al.* Observation of transparency of erbium-doped silicon nitride in photonic crystal nanobeam cavities. *Opt. Express* **18,** 13863–13873 (2010).
87. Gong, Y. *et al.* Linewidth narrowing and Purcell enhancement in photonic crystal cavities on an Er-doped silicon nitride platform. *Opt. Express* **18,** 2601–2612 (2010).
88. Lo Savio, R. *et al.* Enhanced 1.54 μm emission in Y–Er disilicate thin films on silicon photonic crystal cavities. *Opt. Express* **21,** 10278–10288 (2013).
89. Shakoor, A. *et al.* Room temperature all-silicon photonic crystal nanocavity light emitting diode at sub-bandgap wavelengths. *Laser Photon. Rev.* 1–8 (2012).

90. Davies, G. The optical properties of luminescent centres in silicon. *Phys. Rep.* **176,** 83–188 (1989).
91. Recht, D., Capasso, F. & Aziz, M. J. On the temperature dependence of point-defect-mediated luminescence in silicon. *Appl. Phys. Lett.* **94,** 251113 (2009).
92. Lo Savio, R. *et al.* Room-temperature emission at telecom wavelengths from silicon photonic crystal nanocavities. *Appl. Phys. Lett.* **98,** 201106 (2011).
93. Liu, J. *et al.* High-performance, tensile-strained Ge p–i–n photodetectors on a Si platform. *Appl. Phys. Lett.* **87,** 103501 (2005).
94. Geis, M. W. *et al.* CMOS-compatible all-Si high-speed waveguide photodiodes with high responsivity in near-infrared communication band. *IEEE Photon. Technol. Lett.* **19,** 152–154 (2007).
95. Iwamoto, S. & Arakawa, Y. Enhancement of light emission from silicon by utilizing photonic nanostructures. *IEICE Trans. Electron.* **E95-C**, 206–212 (2012).
96. Zhao, J., Wang, A., Green, M. A. & Ferrazza, F. Novel 19.8% efficient 'honeycomb' textured multicrystalline and 24.4% monocrystalline silicon solar cells. *Appl. Phys. Lett.* **73,** 1991–1993 (1998).
97. Shockley, W. & Queisser, H. J. Detailed balance limit of efficiency of p–n junction solar cells. *J. Appl. Phys*. **32,** 510–519 (1961).
98. Polman, A. & Atwater, H. A. Photonic design principles for ultra-high efficiency photovoltaics. *Nature Mater.* **11,** 174–177 (2012).
99. Nozik, A. J. Quantum dot solar cells. *Physica E* **14,** 115–120 (2002).
100. Govoni, M., Mari, I. & Ossicini, S. Carrier multiplication between interacting nanocrystals for fostering silicon-based photovoltaics. *Nature Photon.* **6,** 672–679 (2012).
101. Liu, C-Y., Holman, Z. C. & Kortshagen, U. R. L. Optimization of Si NC/P3HT hybrid solar cells. *Adv. Funct. Mater*. **20,** 2157–2164 (2010).
102. Mangolini, L., Thimsen, E. & Kortshagen, U. High-yield plasma synthesis of luminescent silicon nanocrystals. *Nano Lett.* **5,** 655–659 (2005).
103. Jurbergs, D., Rogojina, E., Mangolini, L. & Kortshagen, U. Silicon nanocrystals with ensemble quantum yields exceeding 60%. *Appl. Phys. Lett.* **88,** 233116 (2006).
104. Gupta, A., Swihart, M. T. & Wiggers, H. Luminescent colloidal dispersion of silicon quantum dots from microwave plasma synthesis: Exploring the photoluminescence behavior across the visible spectrum. *Adv. Funct. Mater.* **19,** 696–703 (2009).
105. Niesar, S. *et al*. Low-cost post-growth treatments of crystalline silicon nanoparticles improving surface and electronic properties. *Adv. Funct. Mater.* **22,** 1190–1198 (2012).
106. Nozik, A. J. Spectroscopy and hot electron relaxation dynamics in semiconductor quantum wells and quantum dots. *Annu. Rev. Phys. Chem.* **52,** 193–231 (2001).
107. Kelzenberg, M. D. *et al.* Photovoltaic measurements in single-nanowire silicon solar cells. *Nano Lett.* **8,** 710–714 (2008).
108. Tian, B., Kempa, T. J. & Lieber, C. M. Single nanowire photovoltaics. *Chem. Soc. Rev*. **38,** 16–24 (2009).
109. Kelzenberg, M. D. *et al.* Enhanced absorption and carrier collection in Si wire arrays for photovoltaic applications. *Nature Mater.* **9,** 239–244 (2010).
110. Kayes, M., Atwater, H. A. & Lewis, N. S. Comparison of the device physics principles of planar and radial p–n junction nanorod solar cells. *J. Appl. Phys.* **97,** 114302 (2005).
111. Kempa, T. J. *et al.* Single and tandem axial *p–i–n* nanowire photovoltaic devices. *Nano Lett.* **8,** 3456–3460 (2008).
112. Mohite, A. D. *et al.* Highly efficient charge separation and collection across *in situ* doped axial VLS-grown Si nanowire p–n junctions. *Nano Lett.* **12,** 1965–1971 (2012).
113. Tian, B. *et al.* Coaxial silicon nanowires as solar cells and nanoelectronic power sources. *Nature* **449,** 885–890 (2007).
114. Bronstrup, G. *et al.* Optical properties of individual silicon nanowires for photonic devices. *ACS Nano* **4,** 7113–7122 (2010).
115. Stelzner, T. *et al.* Silicon nanowire-based solar cells. *Nanotechnology* **19,** 295203 (2008).
116. Christiansen, S. *et al.* Nanowire device concepts for thin film photovoltaics in *Renewable Energy and the Environment Optics and Photonics Congress* OSA Technical Digest (online) (OSA, 2012).
117. Schaller, R. D., Sykora, M., Pietryga, J. M. & Klimov, V. I. Seven excitons at the cost of one: Redefining the limits for conversion efficiency of photons into charge carriers. *Nano Lett*. **6,** 424–429 (2006).
118. Beard, M. C. *et al.* Multiple exciton generation in colloidal silicon nanocrystals. *Nano Lett.* **7,** 2506–2512 (2007).
119. Trinh, M. T. *et al*. In spite of recent doubts carrier multiplication does occur in PbSe nanocrystals. *Nano Lett*. **8,** 1713–1718 (2008).
120. Beard, M. C. *et al*. Comparing multiple exciton generation in quantum dots to impact ionization in bulk semiconductors: implications for enhancement of solar energy conversion. *Nano Lett.* **10,** 3019–3027 (2010).
121. Hanna, M. C. & Nozik, A. J. Solar conversion efficiency of photovoltaic and photoelectrolysis cells with carrier multiplication absorbers. *J. Appl. Phys.* **100,** 074510 (2006).
122. Trinh, M. T. *et al.* Experimental investigation and modeling of Auger recombination in silicon nanocrystals. *J. Phys. Chem. C* **117,** 5963–5968 (2013).
123. Timmerman, D., Izzedin, I., Stallinga, P., Yassievich, I. N. & Gregorkiewicz, T. Space-separated quantum cutting with Si nanocrystals for photovoltaic applications. *Nature Photon*. **2,** 105–109 (2008).
124. Timmerman, D., Valenta, J., Dohnalová, K., de Boer, W. D. A. M. & Gregorkiewicz, T. Step-like enhancement of luminescence quantum yield of Si nanocrystals. *Nature Nanotech*. **6,** 710–713 (2011).
125. Trinh, M. T. *et al.* Direct generation of multiple excitons in adjacent silicon nanocrystals revealed by induced absorption. *Nature Photon.* **6,** 316–320 (2012).
126. Brewer, A. & Von Haeften, K. *In situ* passivation and blue luminescence of silicon clusters using a cluster beam/H_2O codeposition production method. *Appl. Phys. Lett*. **94,** 261102 (2009).
127. Tsybeskov, L., Vandyshev, J. V. & Fauchet, P. Blue emission in porous silicon: Oxygen-related luminescence. *Phys. Rev. B* **49,** 7821–7824 (1994).
128. Guang, S. H. *et al.* Two- and three-photon absorption and frequency upconverted emission of silicon quantum dots. *Nano Lett.* **8,** 2688–2692 (2008).
129. Atwater, H. A. & Polman, A. Plasmonics for photovoltaic devices. *Nature Mater.* **9,** 205–213 (2010).
130. Yablonovitch, E. Statistical ray optics. *J. Opt. Soc. Am*. **72,** 899–907 (1982).
131. Campbell, P. & Green, M. A. Light trapping properties of pyramidally textured surfaces. *J. Appl. Phys.* **62,** 243–249 (1987).
132. Bozzola, A., Liscidini, M. & Andreani, L. C. Photonic light-trapping versus Lambertian limits in thin film silicon solar cells with 1D and 2D periodic patterns. *Opt. Express* **20**, A224–A244 (2012).
133. Oh, J., Yuan, H.-C. & Branz, H. M. An 18.2%-efficient black-silicon solar cell achieved through control of carrier recombination in nanostructures. *Nature Nanotech*. **7,** 743–748 (2012).
134. Otto, M. *et al.* Conformal transparent conducting oxides on black silicon. *Adv. Mater.* **22,** 5035–5038 (2010).
135. Kuo, M.-L. *et al.* Realization of a near-perfect antireflection coating for silicon solar utilizations. *Opt. Lett.* **33,** 2527–2529 (2008).
136. Kroll, M. *et al.* Employing dielectric diffractive structures in solar cells—a numerical study. *Phys. Stat. Sol. (a)* **205,** 2777–2795 (2008).
137. Martins, E. R. *et al.* Deterministic quasi-random nanostructures for photon control. *Nature Commun*. **4,** 2665 (2013).
138. Miller, O. D., Ganapati, V. & Yablonovitch, E. Inverse design of a nano-scale surface texture for light trapping. *Conference on Lasers and Electro-Optics (CLEO)* OSA Technical Digest (online) (OSA, 2012).
139. Vynck, K., Burresi, M., Riboli, F. & Wiersma, D. S. Photon management in two-dimensional disordered media. *Nature Mater.* **11,** 1017–1022 (2012).
140. Oskooi, A. *et al.* Partially disordered photonic-crystal thin films for enhanced and robust photovoltaics. *Appl. Phys. Lett.* **100,** 181110 (2012).
141. Kowalczewski, P., Liscidini, M. & Andreani, L. C. Engineering Gaussian disorder at rough interfaces for light trapping in thin-film solar cells. *Opt. Lett.* **37,** 4868–4870 (2012).
142. Mallick, S. B., Agrawal, M. & Peumans, P. Optimal light trapping in ultra-thin photonic crystal crystalline silicon solar cells. *Opt. Express* **18,** 5691–5706 (2010).
143. Demésy, G. & John, S. Solar energy trapping with modulated silicon nanowire photonic crystals. *J. Appl. Phys.* **112,** 074326 (2012).
144. Martins, E. R., Li, J., Liu, Y. & Krauss, T. F. Engineering gratings for light trapping in photovoltaics: The supercell concept. *Phys. Rev. B* **86,** 041404(R) (2012).
145. Yu, Z., Raman, A. & Fan, S. Fundamental limit of nanophotonic light trapping in solar cells. *Proc. Natl Acad. Sci. USA* **107,** 17491–17496 (2010).
146. Mallik, S. B. *et al.* Ultrathin crystalline-silicon solar cells with embedded photonic crystals. *Appl. Phys. Lett.* **100,** 053113 (2012).
147. Otto, M. *et al.* Extremely low surface recombination velocities in black silicon passivated by atomic layer deposition. *Appl. Phys. Lett.* **100,** 191603 (2012).
148. Paetzold, U. W., Moulin E., Pieters, B. E., Rau, U. & Carius, R. Optical simulations of microcrystalline silicon solar cells applying plasmonic reflection grating back contacts. *J. Photon. Energy* **2,** 027002 (2012).
149. Sai, H., Saito, K., Hozuki, N. & Kondo, M. Relationship between the cell thickness and the optimum period of textured back reflectors in thin-film microcrystalline silicon solar cells. *Appl. Phys. Lett.* **102,** 053509 (2013).
150. Kanzawa, Y. *et al.* Size-dependent near-infrared photoluminescence spectra of Si nanocrystals embedded in SiO_2 matrix. *Solid State Commun.* **7,** 533–537 (1997).
151. Iacona, F., Bongiorno, C., Spinella, C., Boninelli, S. & Priolo, F. Formation and evolution of luminescent Si nanoclusters produced by thermal annealing of SiO_x films. *J. Appl. Phys.* **95,** 3723 (2004).
152. Zacharias, M. *et al.* Size-controlled highly luminescent silicon nanocrystals: A SiO/SiO_2 superlattice approach. *Appl. Phys. Lett.* **80,** 661–663 (2002).

153. Belomoin, G., Therrien, J. & Nayfeh, M. Oxide and hydrogen capped ultrasmall blue luminescent Si nanoparticles. *Appl. Phys. Lett.* **77,** 779–181 (2000).
154. Valenta, J. *et al.* Colloidal suspensions of silicon nanocrystals: from single nanocrystals to photonic structures. *Opt. Mater.* **27,** 1046–1049 (2005).
155. Doğan, I. *et al.* Ultrahigh throughput plasma processing of free standing silicon nanocrystals with lognormal size distribution. *J. Appl. Phys.* **113,** 134306 (2013).
156. Veinot, J. G. C. Synthesis, surface functionalization, and properties of freestanding silicon nanocrystals. *Chem. Commun.* 4160–4168 (2006).
157. Yang, C.-S. *et al.* Synthesis of alkyl-terminated silicon nanoclusters by a solution route. *J. Am. Chem. Soc.* **121,** 5191–5195 (1999).
158. Kim, B. J. *et al.* Kinetics of individual nucleation events observed in nanoscale vapor–liquid–solid growth. *Science* **322,** 1070–1073 (2008).
159. Peng, K. *et al.* Aligned single-crystalline Si nanowire arrays for photovoltaic applications. *Small* **1,** 1062–1067 (2005).
160. Delerue, C. & Lannoo, M. *Nanostructures: Theory and Modelling* (Springer, 2004).
161. Harrison, P. *Quantum Wells, Wires and Dots* 2nd edn (Wiley, 2005).
162. Luppi, M. & Ossicini, S. *Ab initio* study on oxidized silicon clusters and silicon nanocrystals embedded in SiO_2: Beyond the quantum confinement effect. *Phys. Rev. B* **71,** 035340 (2005).
163. Fujii, M., Toshikiyo, K., Takase, Y., Yamaguchi, Y. & Hayashi, S. Below bulk-band-gap photoluminescence at room temperature from heavily P- and B-doped Si nanocrystals. *J. Appl. Phys.* **94,** 1990–1995 (2003).
164. Rosso-Vasic, M., Spruijt, M., van Lagen, B., De Cola, L. & Zuilhof, H. Alkyl-functionalized oxide-free silicon nanoparticles: Synthesis and optical properties. *Small* **4,** 1835–1841 (2008).
165. Kovalev, D., Heckler, H., Polisski, G. & Koch, F. Optical properties of Si nanocrystals. *Phys. Status Solidi B* **215,** 871–932 (1999).
166. Sychugov, I., Juhasz, R., Valenta, J. & Linnros, J. Narrow luminescence linewidth of a silicon quantum dot. *Phys. Rev Lett.* **94,** 087405 (2005).
167. Bruhn, B., Valenta, J., Sychugov, I., Mitsuishi, K. & Linnros, J. Transition from silicon nanowires to isolated quantum dots: Optical and structural evolution. *Phys. Rev. B* **87,** 045404 (2012).
168. Hao, X. *et al.* Effects of boron doping on the structural and optical properties of silicon nanocrystals in a silicon dioxide matrix. *Nanotechnology* **19,** 424019 (2008).
169. Iori, F. & Ossicini, S. Effects of simultaneous doping with boron and phosphor on the structural, electronic and optical properties of silicon nanostructures. *Physica E* **41,** 939 (2009).
170. Fukuda, M., Fujii, M. & Hayashi, S. Room-temperature below bulk-Si band gap luminescence from P and B co-doped and compensated Si nanocrystals. *J. Lum.* **131,** 1066–1069 (2011).
171. Pitanti, A. *et al.* Energy transfer mechanism and Auger effect in Er^{3+} coupled silicon nanoparticle samples *J. Appl. Phys.* **108,** 053518 (2010).
172. Notomi, M. *et al.* Extremely large group-velocity dispersion of line-defect waveguides in photonic crystal slabs. *Phys. Rev. Lett.* **87,** 253902 (2001).
173. Tran, N. V. Q., Combrié, S. & De Rossi, A. Directive emission from high-*Q* photonic crystal cavities through band folding. *Phys. Rev. B* **79,** 041101(R) (2009).
174. Portalupi, S. L. *et al.* Planar photonic crystal cavities with far-field optimization for high coupling efficiency and quality factor. *Opt. Express* **18,** 16064–16073 (2010).

Acknowledgements

We thank L. C. Andreani for his active collaboration and for a critical reading of this manuscript. F.P. acknowledges collaboration on silicon nanostructures, partly reviewed here, with S. Boninelli, G. Franzò, F. Iacona, A. Irrera and M. Miritello. T.G. acknowledges financial support by Technologiestichting STW and Stichting der Fundamenteel Onderzoek der Materie (FOM). M.G. acknowledges D. Gerace and L. C. Andreani for their collaboration on silicon photonic crystals. T.F.K. acknowledges support by the UK EPSRC through EP/F001622/1 "UK Silicon Photonics". F.P., M.G. and T.F.K. acknowledge support by the EU through the NanoScience–ERA project EP/H00680X/1 "LECSIN". F.P. acknowledges partial support by the EU and MIUR through the projects PON01_01725 named "Novel PV Technologies", PON02_00355_3391233 named Energetic, and PON a3_00136 named BRIT.

Additional information

Reprints and permissions information is available online at www.nature.com/reprints. Correspondence should be addressed to F.P.

Competing financial interests

The authors declare no competing financial interests.